THE INELASTIC REACTION $\pi N \to \pi\pi N$ IN THE RESONANCE REGION*(#'s 289, 666, 871)

Presented by G. Smadja
Lawrence Berkeley Laboratory
Berkeley, California

Despite previous attempts[1] to understand the inelastic reaction $\pi N \to \pi\pi N$, our knowledge of this interaction in the resonance region is still very crude. This is enough of a justification to study further a process which accounts for one half of the total πN cross section. Furthermore, the branching ratios of the main resonances into various quasi-two-body channels ($\pi\Delta$, ρN, σN) should shed some light on their origin.

Three papers have been submitted on this subject, covering different center-of-mass energy ranges:

- a Riverside-LBL collaboration[2] with 40,000 events, $\pi^+ p$ (1.8 → 2.1 GeV)
- a Dubna group[3] with ~6,000 events (1 energy) $\pi^- p$ (~1.45 GeV)
- a LBL-SLAC collaboration[4] ~200,000 events $\pi^\pm p$ (1.3 → 1.9 GeV).

In this discussion, I shall rely almost entirely on the last work which covers a wider range, and with which I am more familiar as a co-author. In fact, the results given by all groups are compatible. The data used in the LBL-SLAC study has been gathered from several experiments listed in Table I. Most of these laboratories are pursuing their own analysis.

Table I

Experiments Used in the LBL-SLAC Analysis

Laboratory	Energy Range $\sqrt{s}$ (GeV)	Number of Events $\pi^+\pi^-n$	$\pi^-\pi^0 p$
SLAC-LBL	1.47 → 1.50	1010	648
	1.65 → 1.97	41175	27946
Oxford	1.31 → 1.54	12502	5892
Saclay	1.39 → 1.53	13340	7314
Total	1.31 → 1.97	74027	41800

Laboratory	Energy Range $\sqrt{s}$ (GeV)	$\pi^+\pi^0 p$	$\pi^+\pi^+ n$
Oxford	1.43 → 1.56	7262	1374
Riverside-LBL	1.82 → 2.09	41412	17255
Saclay	1.64 → 1.97	11522	3382
Total	1.43 → 2.09	60196	22011

Model and Assumptions

The description of the final states involves the isobar approximation, in which the reaction is considered as the superposition of several quasi two-body processes. We can have production

*Work supported by the United States Atomic Energy Commission

of a Δ, ρ, or $\sigma(\pi\pi)_{I=J=0}$. To each of these "particles" is associated a final state enhancement factor $f = e^{i\delta_\ell} \sin \delta_\ell / q^\ell$ where δ is the appropriate phase shift and ℓ the angular momentum. We now define the partial waves T_α for the inelastic reaction by the set of numbers α: LL'IJ $\{^{\Delta}_{\sigma}$ (see Fig. 1) and parametrize these matrix elements at a fixed incident energy as

$$T_\alpha = A_\alpha Q^{L'_\alpha} f_\alpha,$$

where Q is the momentum of the resonant subsystem in the overall center of mass, A_α a smooth function of the mass of the subsystem, and f_α the final-state factor. We approximate A_α by a constant: the partial wave amplitude. Several approaches are possible from here on:

1. Without any other hypothesis, one can select a slice of the Dalitz plot involving one specific process and perform a standard quasi two-body analysis. Such a method was used by the LBL-Riverside group[2] with the advantages of simplicity, and possibly a lesser sensitivity to those final-state interactions which are neglected in the following approaches (such as $N^*_{1/2}$ isobars).

2. One may further assume that the different quasi-two-body amplitudes may be added into $T = T_1 + T_2 + T_3$. Some double counting is present, but small in this expression, and all the events are now used in the fit.

3. Bunyatov et al. introduce as a correction term to the previous description, the rescattering associated with the triangle graph. Such a contribution induces small variations in the A_α

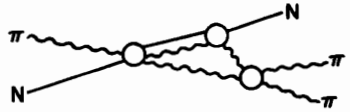

which we have neglected, but when added as a separate term, it obscures the meaning of the partial wave amplitudes. In particular, the comparison with unitarity becomes difficult.

The Fitting Method

The LBL-Riverside group performed energy-dependent fits to the data, but most of the other analyses are done energy by energy. Various binnings of the events together with a χ^2 test minimization (as in Ref. 1) do not take correlations into account as efficiently as the maximum likelihood method chosen by the LBL-SLAC collaboration. A special optimization routine is, however, needed in the latter case. The program was able to treat up to 60 waves. We shall now briefly describe how a "unique" solution is obtained using the likelihood technique, while other analyses were left with ambiguities.

We started from a set of 60 partial waves representing all possible sets of quantum numbers with an orbital angular momentum of the final subsystem $L' \leq 3$. At each of the 17 energy bins, with ~14,000 events at each energy, the 15 best from a set of 2,000 random searches were chosen as starting values in the optimization program. By eliminating waves that were compatible with zero at several adjacent energies, checking for continuity and comparing the likelihoods, we obtained a small subset of significant amplitudes. The number of "necessary" waves increases from 10 (at ~1.3 GeV) to 24 (at 1.9 GeV) and the solution is unique within this subset. We checked that no major wave could be removed without a dramatic worsening of the fit. On the other hand, when an amplitude which is within 1 or 2 standard deviations from zero is taken out or replaced by another one, other waves change by less than a standard deviation.

How Good Are The Fits?

1. Histograms of Masses and Angles

The $N\pi$, $\pi\pi$ mass spectra are well reproduced. Small systematic shifts are, however, present in Fig. 2, which we were unable to cure by adjustments of the isobar mass.

The production angle of the nucleon, θ, is shown in Fig. 3. As the energy increases, so does the backward peak. We do not account fully for this peripheral effect within our waves: higher partial waves would be needed at the end of our energy range.

2. Cross Sections

The cross sections for $\pi^- p \to \pi^+ \pi^- n$, $\pi^- p \to \pi^- \pi^0 p$, $\pi^+ p \to \pi^+ \pi^0 p$ are included in the fitting procedure. The predicted $n\pi^0\pi^0$ cross section shown in Fig. 4 is also in agreement with the measured values over the whole energy range. The fit fails completely, however, for $n\pi^+\pi^+$, finding less than 1/2 of the measured cross section. This is probably tied to the strong presence of $N^*_{1/2}(1520)$, $N^*_{1/2}(1680)$ in this channel.

3. Comparison with Elastic Phase Shift Analyses (EPSA)

Below 1.55 GeV, the total inelasticity of each πN wave is accounted for by our results for $N\pi\pi$, except in the case of S11 where the $\pi N \to \eta N$ channel is important. At higher energies, we always satisfy the unitarity bound, but miss a large part of the inelastic cross section in some isospin 3/2 amplitudes such as F37 and D35. This difficulty may again be related to the omission of $N^*_{1/2}$ resonances in the final-state interactions.

Argand Plots

At each energy, the inelastic waves are only defined up to an overall phase. A K matrix fit described below yielded this phase which allows us to display the various amplitudes on Argand plots. We show the behavior of the channels coupled to the πN waves P11, P13 on Fig. 5(a) and 5(b). D13 is described in the talk of C. Lovelace.[5]

We see clearly resonant-like loops which are not always as apparent in the elastic amplitudes: D13 with the second resonance around 1700, P13 and the broad effect in ρN at ~1800 are striking examples, but a K-matrix analysis is necessary to have quantitative information about the pole position.

K-Matrix Parametrizations

Once the energy-independent solutions have been obtained, we perform in a second stage of the analysis a multichannel K matrix fit in each subspace of IJ^P (isospin, total angular momentum, parity).

Seven channels* are possible in principle: πN, $\pi\Delta_1$, $\pi\Delta_2$, $N\rho_{1/2}$, $(N\rho_{3/2})_1$, $(N\rho_{3/2})_2$,** $N\sigma$, but we never have to deal with more than five in practice. The reduced K matrix is parametrized as

---

*Two $\pi\Delta$ (or $\rho_{3/2}N$) waves, with L' differing by 2, can be present in each I, J^P subspace.

**$\rho_{1/2}$, $\rho_{3/2}$ refer to the two possible couplings of ρ and N spins.

$$K = K_0 + \sum_r \frac{K^r}{s - s_r}, \qquad K = \begin{array}{c} \\ \pi N \\ \pi\Delta_1 \\ \pi\Delta_2 \\ N\rho \\ \cdot \\ \cdot \\ \cdot \end{array} \begin{bmatrix} \pi N & \pi\Delta_1 & \pi\Delta_2 & N\rho & \cdots \\ & & K \to K & & \end{bmatrix}$$

where $K_{ij}^r = \gamma_i^r \gamma_j^r$. The amplitude T is then computed and resonance positions are defined by the poles of T whenever the K matrix description is satisfactory. Table II summarizes the masses of a few resonances found in this fashion.

Table II

Pole Position (MeV)	P11		P13	D13		D15	F15	F35	F37
K Matrix Pole	1497 ±2	1800 ±6	1754 ±7	1520 ±5	1848 ±30	1685 ±5	1682 ±15	1933 ±30	1930 ±4
T Matrix Pole	1564 -i(150)	1738 -i(125)	1746 -i(175)	1506 -i(78)	1613 -i(67)	1694 -i(80)	1667 -i(82)	1802 -i(138)	1900 -i(178)
Error on Real Part of Pile	5	7	30	4	13	10	8	113	2

The systematic study accomplished shows that smooth partial wave representations of the inelastic reactions can be achieved. Coupling constants to the quasi two-body channels are also being obtained. These results are by no means final. Two defects of the work must be stressed again: a lack of high partial waves and a poor description of $n\pi^+\pi^+$ caused by the neglect of $N^*_{1/2}$ isobars.

Other groups (Oxford, Riverside, Saclay, . . .) have contributed not only to the data used by the LBL-SLAC collaboration, but also to the checks of the programs. They are completing similar analyses, and it is clear that the agreement of several experiments is necessary to establish the results.

I also want to thank all the other authors of the LBL-SLAC collaboration who have helped me in the presentation of this material and especially Professor A. Rosenfeld whose interest in the subject provided a constant stimulation.

References

[1] M. DeBeer et al., Nucl. Phys. B12, 599 (1969); M. G. Bowler et al., Nucl. Phys. B17, 331 (1970); W. Chinowsky et al., Phys. Rev. D2, 1790 (1970); A. D. Brody et al., Phys. Letters 34B, 665 (1971).

[2] U. Mehtani et al., A Partial Wave Analysis of $\pi^+ p \to \pi^0 \Delta^{++}$, UCR 34 P107 B-146 (1972), #666.
[3] S. Bunyatov et al., #871.
[4] D. Herndon et al., Lawrence Berkeley Laboratory Report LBL-1065, SLAC-PUB-1108 (1972); Cashmore et al., #289.
[5] C. Lovelace, these Proceedings.

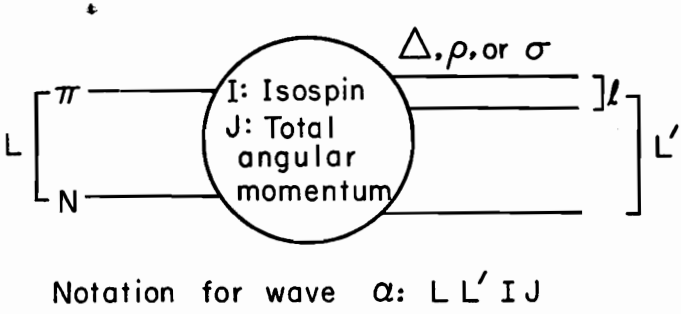

Fig. 1. Definition of the partial waves used in the isobar approximation.

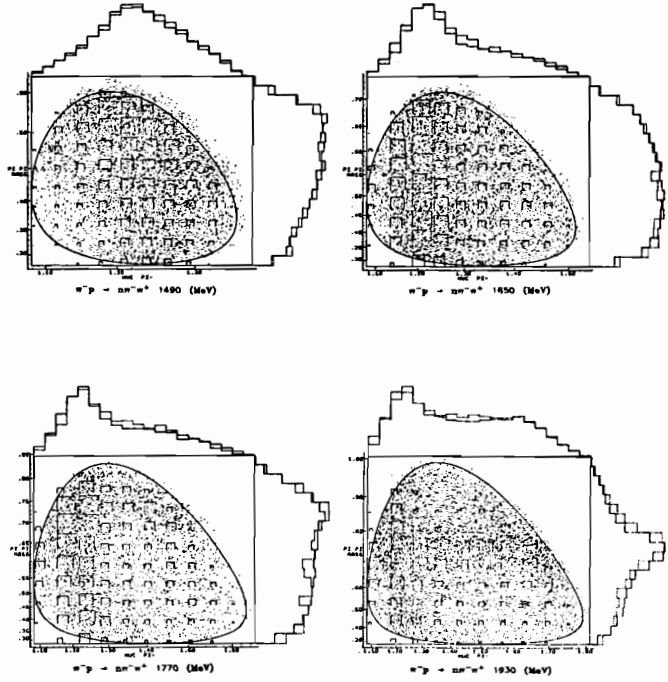

Fig. 2. Dalitz plot and its projections at four energies for the reaction $\pi^- p \to \pi^+ \pi^- n$. The dotted line is the data in the projected spectra while the solid line is the fit. The side of the little squares in the Dalitz plot is proportional to the computed population density.

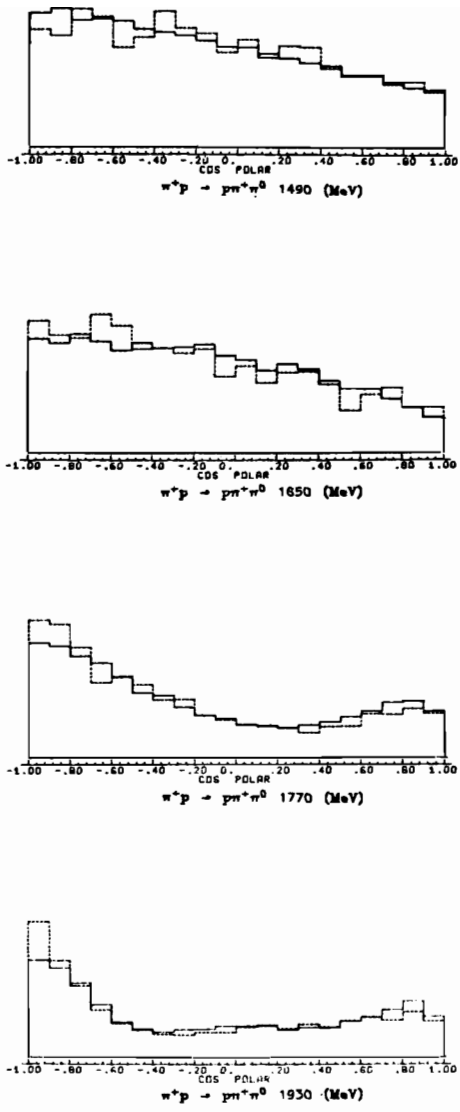

Fig. 3. Distribution of the production angle of the proton in the overall center of mass (with respect to the incoming pion. The dotted line is the data, the solid is the fit.

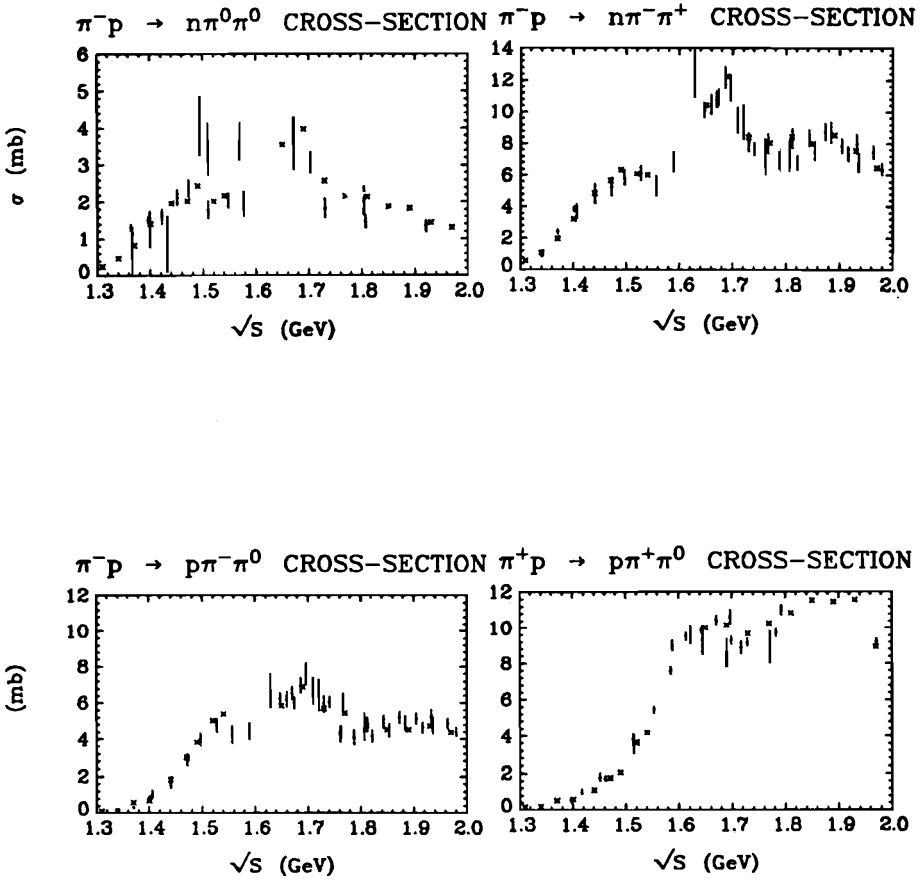

Fig. 4. Comparison of the fitted cross sections (x) with the experimental values.

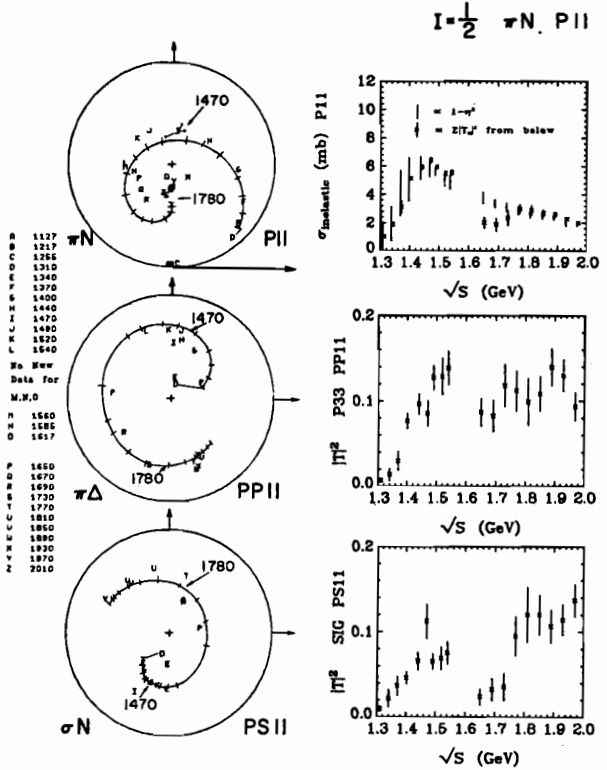

Fig. 5(a)

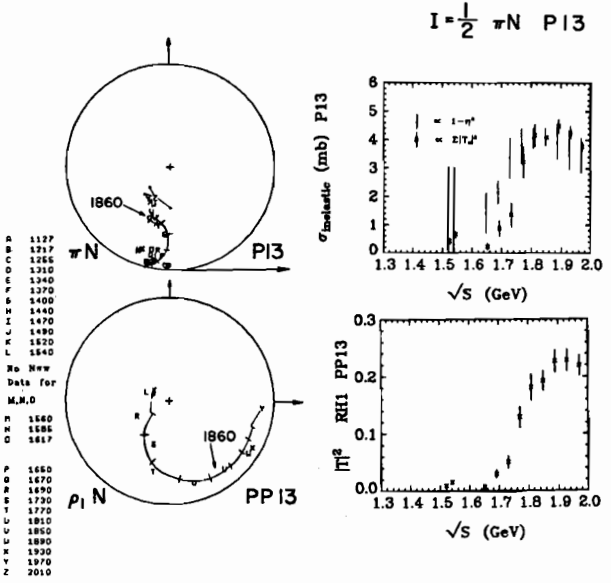

Fig. 5(b)

Fig. 5. On the left, Argand plots for $\pi N \to \pi N$, $\pi N \to (\pi\Delta, \rho N, \sigma N)$ are shown. Letters are the results of the maximum likelihood fit (or EPSA). The curve is the K matrix fit. On the right: inelastic contribution of $N\pi\pi$ in the wave, and partial contribution of each channel ($\pi\Delta$, ρN, . . . etc.) to the cross section. a) P11; b) P13.